Determination of the Quantum Yield for the Photochemical Generation of Hydroxyl Radicals in TiO2 Suspensions

ARTICLE *in* THE JOURNAL OF PHYSICAL CHEMISTRY · MARCH 1996

Impact Factor: 2.78 · DOI: 10.1021/jp9505800

2 AUTHORS, INCLUDING:

James R Bolton
University of Alberta
315 PUBLICATIONS **10,087** CITATIONS

Determination of the Quantum Yield for the Photochemical Generation of Hydroxyl Radicals in TiO_2 Suspensions

Lizhong Sun[†] and James R. Bolton*

Photochemistry Unit, Department of Chemistry, The University of Western Ontario, London, Ontario, Canada N6A 5B7

Received: March 1, 1995[⊗]

The generation of hydroxyl (•OH) radicals plays a key role in the heterogeneous photocatalytic degradation of organic pollutants in aqueous suspensions of TiO_2. The quantum yield of this process is thus an important parameter; however, it is not easy to measure in a particulate system arising from problems caused by light scattering from the particles. In this work, a reliable method for the determination of the quantum yield of hydroxyl radical production in heterogeneous systems has been developed, based on measurements of •OH radical generation rates and the photon flux absorbed by TiO_2 suspensions. In this procedure, a modified integrating sphere method was used to determine the true fraction of light absorbed by TiO_2 suspensions. A ferrioxalate chemical actinometer was used to measure the incident photon flux. As a check on the quantum yield method, good agreement with known literature values was obtained for quantum yield measurements of the photochemical generation of the *p*-benzosemiquinone ($BQ^{\bullet-}$) radical in the photolysis of *p*-benzoquinone and of the •OH radical generation in the photolysis of hydrogen peroxide, respectively. Accordingly, the quantum yield for the •OH radical production in the TiO_2 suspension was determined to be 0.040 ± 0.003 at pH 7. Effects on the quantum yield of suspension loading, photon flux, and electron-acceptor addition (H_2O_2 and O_2) were explored.

1. Introduction

The photocatalytic degradation of pollutants in aqueous solutions is attracting considerable attention for application to environmental problems.[1−3] This is a process in which photoinduced holes in semiconductor particles (such as TiO_2) oxidize hydroxide ions (or water molecules) adsorbed on the surface of the particles to produce highly oxidizing •OH radicals, which subsequently attack adsorbed pollutant molecules. This primary step initiates a series of degradation reactions that ultimately lead to mineralization of the pollutants.

Obviously the quantum yield for the generation of •OH radicals plays a very important role in determining the efficiency of photodegradation of the pollutants. Nevertheless, it has proved difficult to measure this quantum yield in heterogeneous photocatalytic processes because of the problem of light scattering. Perhaps this is why many studies on photocatalysis in heterogeneous systems either do not report quantum yields or just give "apparent" quantum yields based on the incident photon flux.[4−6]

Schiavello et al.[7] developed an experimental method for the detection of the quantity of photons absorbed by aqueous TiO_2 dispersions, in which two parameters, the photon flux reflected and the photon flux absorbed by particle dispersions, were evaluated by measuring the photon flux entering the photoreactor and the photon flux transmitted by the photoreactor. Lepore et al.[8] determined an "apparent" quantum yield of 0.012 for the removal of 4-chlorophenol in a TiO_2 suspension. Using optically transparent preparations of very small TiO_2 particles, they determined a true quantum yield of 0.020 at 313 nm for the oxidation of iodide. For the same TiO_2 suspension they found true quantum yields of 0.2−0.6 for the removal of propanal and speculated that the limiting quantum yield is unity for a very high concentration of propanal. Valladares and Bolton[9] used a special cell, in which an aluminum foil jacket had a small aperture to let in the light, which was then scattered and reflected by the grains, to measure the true quantum yield (0.05) for the bleaching of methylene blue. None of these earlier studies involved the direct determination of the true quantum yield of hydroxyl radical generation but rather focused on the removal of a specific contaminant.

In this work, we have employed methanol to trap •OH radicals produced in the photocatalytic process in TiO_2 suspensions. A modified integrating sphere method was utilized to measure the true fraction of light absorbed in the TiO_2 suspensions. The incident photon flux was measured using the ferrioxalate actinometer. Confirmations of the reliability of the method and the system for quantum yield measurements were carried out for the *p*-benzoquinone (BQ) system and the H_2O_2 system, respectively, and good agreement was obtained with literature values for the quantum yields for both the *p*-benzosemiquinone ($BQ^{\bullet-}$) radical generation and the •OH radical production, respectively. The effects of suspension loading, light flux and electron acceptors (H_2O_2 and oxygen) on the •OH radical quantum yield in TiO_2 were examined.

2. Principles

The quantum yield for a photochemical reaction can be expressed as

$$\phi = \frac{\text{rate of reaction induced by photon absorption}}{\text{flux of absorbed photons}} \quad (1)$$

When photons with an energy greater than the bandgap are absorbed by TiO_2 particles, electrons are promoted from the valence band to the conduction band leaving holes in the valence band. The photoinduced holes migrate to the surfaces of the particles and there react with adsorbed hydroxide ions (or water molecules), producing •OH radicals. At the same time, the

[†] Current address: School of the Environment, Duke University, A141 Science Research Center, Research Drive, Durham, NC 20078.

* To whom correspondence should be addressed.

[⊗] Abstract published in *Advance ACS Abstracts*, February 1, 1996.

0022-3654/96/20100-4127$12.00/0

conduction band electrons reduce oxygen adsorbed on the surfaces to form $O_2^{\bullet-}$ radicals:

$$TiO_2 \xrightarrow{h\nu} e_{cb}^- + h_{vb}^+ \quad (2a)$$

$$h_{vb}^+ + OH^- \rightarrow {}^\bullet OH \quad (2b)$$

$$e_{cb}^- + O_2 \rightarrow O_2^{\bullet-} \quad (2c)$$

The $^\bullet OH$ radical quantum yield ϕ_{OH} can be determined from the generation rate R_{OH} of $^\bullet OH$ radicals and the flux I_a of absorbed photons:

$$\phi_{OH} = R_{OH}/I_a \quad (3)$$

Determination of the $^\bullet OH$ Radical Generation Rate. Hydroxyl radicals are known to react with aliphatic alcohols through abstraction of a hydrogen atom from a C—H bond.[10,11] The method we have used for determining the absolute $^\bullet OH$ radical generation rate is based on α-H atom abstraction by $^\bullet OH$ radicals from methanol (in excess), followed by monitoring of the formation rate of the principal stable product, formaldehyde.[12-15] The reaction is

$$^\bullet OH + CH_3OH \rightarrow {}^\bullet CH_2OH + H_2O \quad (4)$$

In the presence of oxygen, formaldehyde is formed as the dominant stable product in a quantitative reaction ($k = 9.6 \times 10^9$ M^{-1} s^{-1})[16]

$$^\bullet CH_2OH + O_2 \rightarrow HCHO + HO_2^\bullet \quad (5)$$

The formaldehyde generated by reactions 4 and 5 can be measured by HPLC with UV absorbance detection at $\lambda = 360$ nm, after forming its 2,4-dinitrophenylhydrazine (DNPH) derivative:[17]

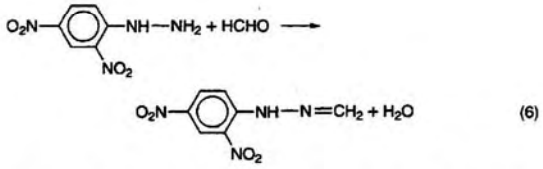

(6)

The hydrogen abstraction of aliphatic alcohols by $^\bullet OH$ radicals had been considered to have a 100% yield;[18,19] however, Burchill and Ginns[20] found that α-H abstraction by $^\bullet OH$ radicals occurs to only 90% and 86% from ethanol and 2-propanol, respectively. Asmus et al.[12] showed that the efficiency of the reaction of $^\bullet OH$ radicals with methanol by α-H abstraction is 93%. The remaining 7% is accounted for by methoxy radicals formed in the reaction

$$^\bullet OH + CH_3OH \rightarrow H_2O + CH_3O^\bullet \quad (7)$$

The concentration of the HCHO derivative, divided by a factor of 0.93, is thus the corresponding $^\bullet OH$ radical concentration produced in the reaction of the H_2O_2 system. The fraction of $^\bullet OH$ radicals that react with methanol to produce HCHO in the TiO_2 system is not available; we make the arbitrary assumption that it has the same value as that found in the homogeneous system (0.93).

Flux of Absorbed Photons. The photon flux I_a absorbed by a sample is the product of the incident photon flux I_o, and for a sample S, the integrated absorption fraction F_S over the wavelength range used in the experiment:

$$I_a = I_o F_S \quad (8)$$

which can be determined photochemically and spectrophotometrically (see Appendix 1).

Final Expression for the Quantum Yield. From eqs 3 and 8 and the derivation in Appendix 1, the final expression for the quantum yield is

$$\phi_S = \frac{R_{OH}}{R_{Fe^{2+}}} \rho_S \phi_{Fe^{2+}} \quad (9)$$

where

$$\rho_S = F_{Fe(III)}/F_S \quad (10)$$

where $F_{Fe(III)}$ is the fraction of light absorbed in the ferrioxalate actinometer solution.

Modified Integrating Sphere Method. The fraction of light absorbed by a sample undergoing a photochemical reaction is an important parameter in a quantum yield measurement. It can easily be calculated from the spectrophotometric absorbance in a homogeneous system. But the determination of the fraction of light absorbed for a heterogeneous suspension is not so easily determined due to light scattering by the particles. In our experiments, we used a modified integrating sphere to determine the fraction of light absorbed in a light-scattering suspension. The sample, in an EPR flat cell (path length 0.33 mm) was placed at the sample position of the integrating sphere with air as the reference. The detailed method and theory of the modified integrating sphere are described in Appendix 2.

3. Experimental Section

Materials. The TiO_2 powder (anatase) was from Aldrich Chemical Co., Inc. The suspension was prepared by sonication, centrifugation, and evaporation to narrow the particle size distribution and to increase the loading of the suspension.[21,22] The loading was measured using a weight method (see ref 23 for details). The TiO_2 particle diameters, measured using scanning electron microscopy (SEM), ranged from 100 to 210 nm. Most suspensions were made in 1.0 mM phosphate buffer solution (BDH).

A 2,4-dinitrophenylhydrazine (DNPH) solution, used for the derivatization of the formaldehyde produced in reaction 6, was made by dissolving 0.475 g of DNPH (Kodak Laboratory & Research Products) in 100 mL of a solution containing concentrated HCl (12 M), water and acetonitrile in the ratio 2:5:1 (v/v/v).

A 0.0398 mM solution of the HCHO derivative of DNPH was used with and without $BaSO_4$ (BDH) particles (loading of the $BaSO_4$ particles was 1.36 g L^{-1}), as a test of the modified integrating sphere method.

A solution of 1.0 mM *p*-benzoquinone (BQ, Fisher Scientific Co.) was used for the measurement of the quantum yield for the *p*-benzosemiquinone ($BQ^{\bullet-}$) generation.

The oxygen concentrations in the suspension were controlled by bubbling a mixture of oxygen and nitrogen at a certain proportion into the suspension until adsorption equilibrium of the oxygen on particles in the suspension was reached.

Double-distilled water was used for the preparation of all the solutions and suspensions.

Photolyses. Photolyses were carried out using a water-filtered 200 W xenon/mercury UV lamp (Oriel Corp. of America) with a UV transmitting black glass filter (365 ± 50 nm, Melles Griot). The transmittance of the UV transmitting black glass filter in the range 300–400 nm was measured by a UV/vis spectrophotometer (Figure 1). The photolysis, both for the $^\bullet OH$ radical measurement with methanol and for the photon

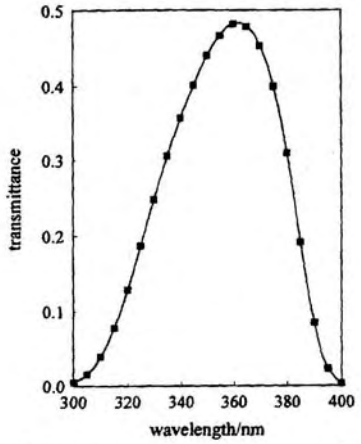

Figure 1. Transmittance spectrum of the UV black transmitting glass filter.

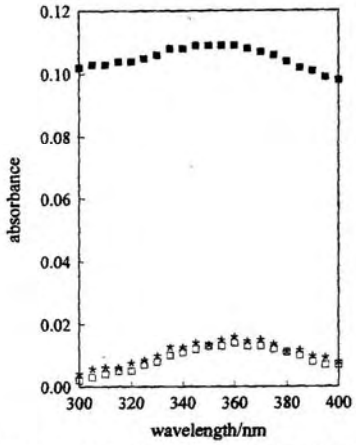

Figure 2. Absorbance of a HCHO derivative solution with and without $BaSO_4$ particles: (■) absorbance of a 3.98×10^{-5} M HCHO−DNPH derivative in the presence of $BaSO_4$ particles, $BaSO_4$ loading = 1.36 g L^{-1}; (□) absorbances of the same solution without $BaSO_4$ particles; (*) absorbance of the solution with $BaSO_4$ particles, as determined using the modified integrating sphere method.

flux determinations, took place in a WG-812 EPR flat sample cell (Wilmad Glass Company, Inc.) at the same light intensity, which are the same conditions as used in our previous work linked with the measurement of the hydroxyl radical trapping efficiency by a spin trap.[23] The cell path length was determined to be 0.33 mm from the absorbance measurement of a 5,5-dimethyl-1-pyrroline *N*-oxide solution (DMPO) of known concentration.

Absorption measurements for the TiO_2 suspensions were determined using an integrating sphere assembly (Shimadzu Corp.) linked with a UV-260 spectrophotometer (Shimadzu Corp.).

HPLC Measurements. The photolyzed solution (1.0 mL) in an EPR flat cell was washed out and diluted to 3 mL final volume and then derivatized by adding 100 μL of the DNPH solution. After sitting for 1.5 h at room temperature (25 °C), an aliquot of the sample was injected into a Waters Model 501 solvent delivery system connected with a μ Bondapak C_{18} column and measured by Waters 486 HPLC tunable absorbance detector set at 360 nm. The derivative was eluted isocratically with 45% acetonitrile aqueous solution as the mobile phase.

All the samples for HPLC measurement were filtered using Millipore films (0.1 μm) before measurement. The data for HCHO derivative measurements are averages of three measurements. The reliability of the HCHO derivative as a measure of the $^{\bullet}OH$ radical generation in the system has been proven in our previous work.[23]

Measurement of the Photon Flux. The photon flux was measured immediately after a photolysis run using potassium ferrioxalate actinometry. The EPR flat cell (0.33 mm path length), containing a 0.15 M ferrioxalate solution, prepared from $K_3Fe(C_2O_4)_3$ (Fisher) recrystallized in the dark, was put into the EPR cavity and irradiated with the UV lamp. The rate of production of ferrous ions $R_{Fe^{2+}}$ was determined by a UV/vis spectrophotometer (Hewlett-Packard Model 8450A) at 510 nm 1 h after addition of 0.1% of 1,10-phenathroline (Aldrich) to the photolyzed solution. The weighted average of the quantum yield of the ferrous ion production from ferrioxalate (0.15 M) over the bandwidth of the black transmitting glass filter is known to be 1.19.[22,24]

Electron Paramagnetic Resonance (EPR) Measurements. EPR spectra of the *p*-benzosemiquinone produced during photolysis of *p*-benzoquinone were obtained using a Bruker Model ESP300 electron paramagnetic resonance spectrometer. The details concerning the EPR measurements can be found in our previous work.[23]

4. Results and Discussion

Fraction of Light Absorbed in the TiO_2 Suspensions. *Check of the Modified Integrating Sphere Method.* As a check of the modified integrating sphere method, the absorbance of a 0.0398 mM solution of the HCHO derivative of DNPH was determined with and without $BaSO_4$ particles (loading of $BaSO_4$ was 1.36 g L^{-1}). Figure 2 shows the marked difference for the suspension with the $BaSO_4$ particles between a normal absorption spectrum (i.e., the absorption spectrum measured with a normal spectrophotometer without using an integrating sphere), and one determined using the modified integrating sphere method. The latter spectrum, which has been corrected for the scattering, is close to that for the solution without $BaSO_4$ suspended particles. This suggests that the modified integrating method effectively eliminates the interference, arising from the scattering light, on the absorption measurement and that the absorption spectrum measured using this method is an accurate representation of the true absorption spectrum of the suspension.

True Absorbance Spectrum of TiO_2. Figure 3 shows a comparison of the apparent absorbance of TiO_2 suspensions using a normal UV spectrophotometer and the true absorbance from the modified integrating sphere method, where eq A11 has been utilized.

The fraction of light absorbed at a given wavelength λ is then obtained from eq A2 in Appendix 1.

Hydroxyl Radical Formation Rates. Figure 4 shows the change of the HCHO derivative concentration as a function of irradiation time in the TiO_2 suspensions. A linear relation of the HCHO derivative concentration with irradiation time was obtained. From this figure the growth rate of HCHO derivative was found to be $(3.16 \pm 0.13) \times 10^{-7}$ M s^{-1}, and thus the $^{\bullet}OH$ radical generation rate is $d[^{\bullet}OH]/dt = (3.40 \pm 0.13) \times 10^{-7}$ M s^{-1}, after applying the 0.93 correction factor.

Confirmation of the Quantum Yield Measurement Method. To confirm the reliability of the method for quantum yield

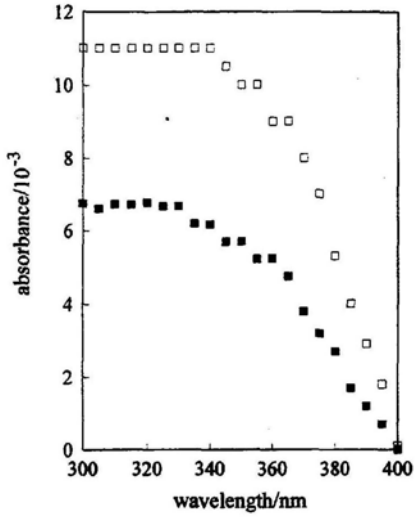

Figure 3. Absorbance spectra of a TiO_2 suspension. Loading of the suspension is 67 mg L^{-1}: (□) uncorrected spectrum in the normal UV/vis measurement; (■) corrected absorption spectrum using the modified integrating sphere method.

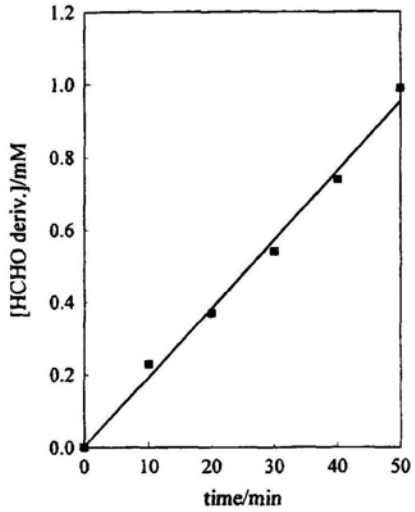

Figure 4. Effect of irradiation time on the concentration of the HCHO derivative in the TiO_2 suspension. Loading of the suspension is 100 mg L^{-1}; $[CH_3OH] = 30.0$ mM.

measurement method, two systems, whose quantum yields are well-known, were tested: the *p*-benzoquinone (BQ) system for the generation of the *p*-benzosemiquinone ($BQ^{\bullet-}$) radial and the H_2O_2 system for the homogeneous generation of $^{\bullet}OH$ radicals.

Quantum Yield of the p-Benzosemiquinone Radical Generation in the BQ System. In an aqueous solution, *p*-benzosemiquinone ($BQ^{\bullet-}$) radicals can be generated through the photolysis of *p*-benzoquinone (BQ):[25]

$$BQ \xrightarrow{h\nu} BQ^{\bullet-} \tag{11}$$

The $BQ^{\bullet-}$ radical has a five-line electron paramagnetic resonance (EPR) spectrum. In a similar manner to eq 9, the quantum yield ϕ_{BQ} for the $BQ^{\bullet-}$ radical generation can be also expressed as

$$\phi_{BQ} = \frac{R_{BQ}\phi_{Fe^{2+}}\rho_{BQ}}{R_{Fe^{2+}}} \tag{12}$$

where R_{BQ} is the generation rate of $BQ^{\bullet-}$ radicals.

R_{BQ} was obtained from the slope of the growth curve of the radicals, when the field was fixed at the peak of the center line of the $BQ^{\bullet-}$ EPR spectrum, using a method similar to that described in our previous work.[23] The coefficient ρ_{BQ} for the BQ solution (cf. eq 10) in the range 300−400 nm was found to be 289 ± 8. The corresponding parameters used for the calculation of the quantum yield are summarized in Table 1. According to the results, the quantum yield of $BQ^{\bullet-}$ radical generation was found to be 0.44 ± 0.05, which is very close to the literature value (0.47 ± 0.04).[25]

Quantum Yield of the $^{\bullet}OH$ Radical Generation in the Homogeneous H_2O_2 System. In the H_2O_2 system, $^{\bullet}OH$ radicals are produced homogeneously by the photolysis of hydrogen peroxide:

$$H_2O_2 \xrightarrow{h\nu} 2^{\bullet}OH \tag{13}$$

The generation rate R_{OH} of $^{\bullet}OH$ radicals in 5.0 mM H_2O_2 solution was measured by using the same method as that used in the TiO_2 suspensions and found to be $(3.60 \pm 0.11) \times 10^{-7}$ M s^{-1}. The absorption fraction $F_{H_2O_2}$ (eq A1 of Appendix 1) of the H_2O_2 solution, based on the absorbance of the solution, was calculated to be 7.79×10^{-4}. Thus, the coefficient $\rho_{H_2O_2}$ of the solution (cf. eq 10) was found to be 1285 ± 11. Corresponding parameters for the calculation of the quantum yield in eq 9 are listed in Table 1. Accordingly, the quantum yield for the $^{\bullet}OH$ radical generation in the homogeneous H_2O_2 system was calculated to be 0.96 ± 0.09, which is consistent with the literature values (0.98 ± 0.03 at 308 nm and 0.96 ± 0.04 at 351 nm) in the wavelength range this experiment involved.[26]

The excellent agreement with literature values for the quantum yields of the two systems examined confirmed that the chosen method for quantum yield measurements is feasible and reliable.

Quantum Yield of $^{\bullet}OH$ Radical Production in TiO_2 Suspensions. The intermediate data for the quantum yield measurement, including the growth rate R_{OH} of $^{\bullet}OH$ radicals, the incident photon flux I_o and the absorption fractions F_S, both for TiO_2 suspension (loading of 100 mg L^{-1}) with 30 mM methanol and for the ferrioxalate actinometry solution, R_{OH}, $R_{Fe^{2+}}$, and ρ are listed in Table 1. The calculation, using eq 9, shows that the quantum yield of the $^{\bullet}OH$ radical generation in the TiO_2 system is 0.040 ± 0.003.

This low value explains why many studies of the photodegradation of pollutants in TiO_2 suspensions show very low quantum yield values for the disappearance of the pollutants or the formation of degradation products, which are processes following the primary generation of $^{\bullet}OH$ radicals. For example, Matthews[27] reported that the "apparent" quantum yield for the disappearance of phenol from a 100 mM solution in 0.1% TiO_2 suspension is ~0.6%; Bahnemann et al.[28] determined that the "apparent" quantum yield of H_2 formation in the illumination of a colloidal TiO_2 solution was about 0.01. Anpo et al.[29] obtained ~0.12% maximum "apparent" quantum yield for the photocatalytic hydrogenolysis of methylacetylene ($CH_3C{\equiv}CH$) with H_2O in the TiO_2 (anatase) particulate system.

Effects of Several Factors on the Quantum Yield. *Loading of the TiO_2 Suspensions.* Table 2 shows quantum yields measured in suspensions with different TiO_2 loadings. The average value of the quantum yield is 0.039 ± 0.003. The results indicate that variation of the loading in a fairly wide

TABLE 1: Intermediate Data in the Quantum Yield Calculations

system	R_s/M s^{-1}	$R_{Fe^{2+}}$/M s^{-1}	$F_{Fe^{2+}}$[a]	F_s[a]	ϱ[b]	ϕ
BQ	$(5.50 \pm 0.38) \times 10^{-7}$	$(4.30 \pm 0.11) \times 10^{-4}$	0.9977	0.0034	289 ± 8	0.44 ± 0.05
H_2O_2	$(3.35 \pm 0.11) \times 10^{-7}$	$(4.56 \pm 0.09) \times 10^{-4}$	0.9977	7.79×10^{-4}	1285 ± 11	0.94 ± 0.05
TiO_2	$(3.16 \pm 0.13) \times 10^{-7}$	$(4.56 \pm 0.09) \times 10^{-4}$	0.9977	0.0172	58 ± 1	0.040 ± 0.003

[a] Calculated using eq A1 of the Appendix for the wavelength range 300−400 nm. [b] Calculated using eq 10.

TABLE 2: Effect of Suspension Loading on Quantum Yield of •OH Radical Generation[a]

loading/mg L^{-1}	R_{OH}/M s^{-1}	$R_{Fe^{2+}}$/M s^{-1}	$F_{Fe^{2+}}$	F_s	ϱ[b]	ϕ
11	$(3.59 \pm 0.18) \times 10^{-8}$	$(4.56 \pm 0.09) \times 10^{-4}$	0.9977	0.0021	480 ± 6	0.038 ± 0.003
22	$(7.40 \pm 0.35) \times 10^{-8}$	$(4.56 \pm 0.09) \times 10^{-4}$	0.9977	0.0042	238 ± 4	0.039 ± 0.003
44	$(1.37 \pm 0.03) \times 10^{-7}$	$(4.56 \pm 0.09) \times 10^{-4}$	0.9977	0.0082	121 ± 2	0.036 ± 0.002
67	$(2.15 \pm 0.09) \times 10^{-7}$	$(4.56 \pm 0.09) \times 10^{-4}$	0.9977	0.0119	84 ± 2	0.034 ± 0.003
100	$(3.16 \pm 0.13) \times 10^{-7}$	$(4.56 \pm 0.09) \times 10^{-4}$	0.9977	0.0172	58 ± 1	0.040 ± 0.003
150	$(3.32 \pm 0.16) \times 10^{-7}$	$(4.56 \pm 0.09) \times 10^{-4}$	0.9977	0.0184	54 ± 2	0.039 ± 0.004
225	$(3.42 \pm 0.16) \times 10^{-7}$	$(4.56 \pm 0.09) \times 10^{-4}$	0.9977	0.0192	52 ± 1	0.039 ± 0.003
325	$(3.49 \pm 0.17) \times 10^{-7}$	$(4.56 \pm 0.09) \times 10^{-4}$	0.9977	0.0196	51 ± 1	0.039 ± 0.003

[a] See footnotes to previous table.

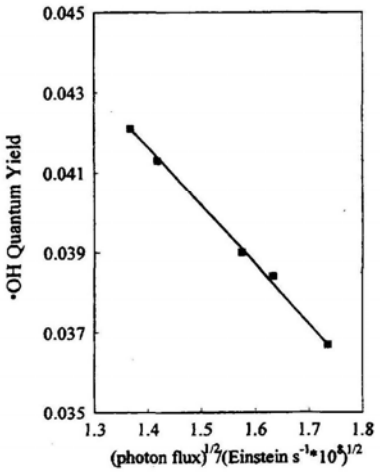

Figure 5. Dependence of the quantum yield on the photon flux. TiO_2 loading is 100 mg L^{-1}.

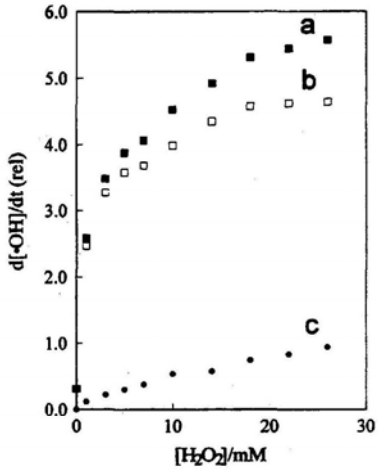

Figure 6. Effect of H_2O_2 addition on the •OH radical generation rate: (a) TiO_2 suspension + H_2O_2; TiO_2 loading is 100 mg L^{-1}; (c) H_2O_2 only; (b) difference of curves a and c.

range (from 11 to 325 mg L^{-1}) does not alter the measured quantum yield. This seems reasonable; according to eq 9, when the loading of a suspension is high, the flux of absorbed photons is larger, which generates more •OH radicals, that is, the generation rate of •OH radicals R_{OH} increases. It is notable that in Table 2 the increase of R_{OH} and the decrease of the coefficient ρ_{OH} of the TiO_2 suspensions are in about same proportion, resulting in an invariant quantum yield.

Photon Flux. Figure 5 shows the relation of the quantum yield with *incident* photon flux I_o. It indicates that the quantum yield decreases with increasing incident photon flux. This is because increasing the incident photon flux level increases the production rate of electron−hole pairs, which increases the opportunity for electron−hole recombination, that is, it decreases the relative number of the photoinduced carriers taking part in the redox reaction on the surface. This results in a decrease of the quantum yield when the photon flux is high.[30] The measurements indicate that the quantum yield is inversely proportional to the square root of the incident photon flux level, which is consistent with the result reported by Kormann et al.[31] in a study of the photocatalytic degradation of chloroform in aqueous suspensions of TiO_2. This suggests that the incident photon flux level used in the experiment was in the limiting range for the induction of carriers in the particles.

Reduction Process. The basic redox reactions that take place on the surfaces of TiO_2 particles are given in eqs 2b and 2c. As a redox process, the consumption rates of holes and electrons should be equal. But usually, on reaching the surface of the particles, holes react with species adsorbed there much faster than electrons.[32] Therefore, kinetically eq 2c is considered as a rate-controlling process. Accordingly, any methods that can influence the rate of eq 2c, such as competing for electrons with oxygen, that is, by adding electron acceptors into the suspension (e.g., hydrogen peroxide) or by increasing the concentration of oxygen, can promote the reduction process, avoid an accumulation of the electrons on the particles (i.e., reduce the recombination rate), and thus increase the rate of the whole redox process, which increases the quantum yield.

Addition of H_2O_2 as an Electron Acceptor. Figure 6 shows the effect of different concentrations of H_2O_2 on the generation rate of •OH radicals in the TiO_2 suspension. In the figure, curve a is the case of the TiO_2 suspension with H_2O_2; curve c is the case of a homogeneous solution with same concentrations of H_2O_2 as in curve a but without TiO_2 particles; and curve b is the difference between curves a and c, which represents the net effect on the generation rate of the •OH radicals by the addition of H_2O_2 to the suspension. Accordingly, the effect of H_2O_2

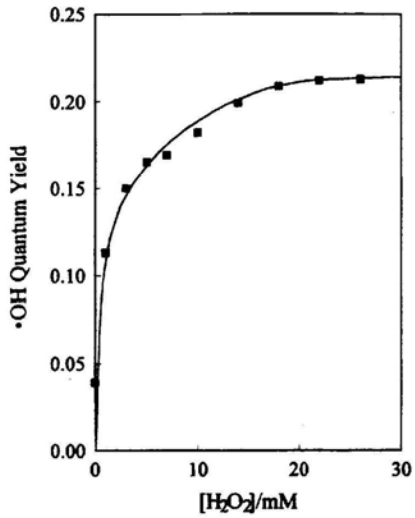

Figure 7. Effect of H_2O_2 addition on the quantum yield; TiO_2 loading is 100 mg L^{-1}.

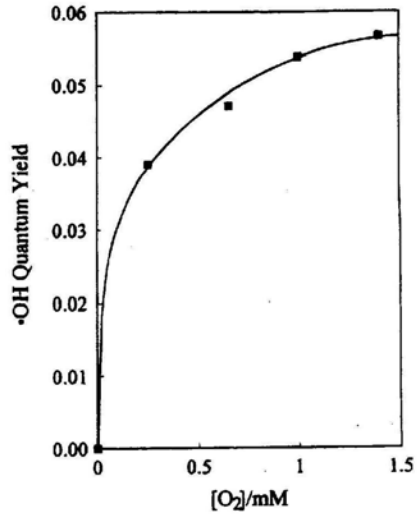

Figure 8. Effect of oxygen concentration on the quantum yield; TiO_2 loading is 100 mg L^{-1}.

addition on the quantum yield of •OH radical production was obtained. Because the reduction of H_2O_2 by a conduction band electron generates one additional •OH radical for every one produced by oxidation of water in reaction 2b, the measured •OH radical generation in the presence of the H_2O_2 radical generation was divided by a factor of 2 to obtain the real generation rate of the •OH radicals produced by photoinduced holes from the semiconductor particles. The quantum yields in the case of the addition of the H_2O_2 in Figure 7 were calculated in this manner. Note that these quantum yields in the presence of H_2O_2 are lower limits because we have assumed that all of the incident UV light is available for the direct photolysis of H_2O_2; in fact, some is absorbed by the TiO_2.

Figure 7 indicates that the addition of the H_2O_2 to the suspension can dramatically increase the quantum yield of •OH radical generation (from 0.040 to 0.22). When the H_2O_2 concentration in the suspension is larger than 18 mM, a plateau is reached.

An explanation of the above results is that the presence of the H_2O_2 in the suspension can influence the redox reactions happening on the surfaces of the particles. In the process, the added H_2O_2 acts as an electron acceptor, which competes with O_2 in the redox reactions and produces additional •OH radicals at the same time:

$$H_2O_2 + e_{cb}^- \rightarrow {}^{\bullet}OH + OH^- \qquad (14)$$

The competition of the H_2O_2 with O_2 for conduction band electrons speeds up the reaction process and the whole redox process, so as to increase the generation rate of •OH radicals. Hence, the quantum yield of •OH radical generation is greatly increased.

We can now understand the reason for the increases of degradation rates of organic pollutants by the addition of H_2O_2, which were reported by some researchers in several TiO_2 suspension systems.[36,37] Our work now confirms that this is the result of the increase of the quantum yield for •OH radical production in these systems.

The plateau in the high H_2O_2 concentration region (> 18 mM) perhaps indicates that a limiting reaction rate has been reached in the system, perhaps due to reaction of hydroxyl radicals with H_2O_2.[38]

Effect of the Oxygen Concentration. As mentioned above, in redox eqs 2b and 2c, the reduction reaction is a rate-controlling step. Therefore, oxygen, as an electron acceptor, can affect the efficiency of spontaneous photoelectrochemical processes on semiconductor particles. Figure 8 shows the effect of oxygen concentration in suspensions on the quantum yield of the •OH radical generation. The experimental results indicate that the higher the content of dissolved oxygen in the suspension, which is in equilibrium with the oxygen adsorbed on the particles in the suspension, the larger the quantum yield. This means that the redox reaction on the surface of the particles is moderately influenced by the quantity of O_2 adsorbed on the TiO_2 particle surfaces. Okamoto et al.[39] found a similar increase of the initial reaction rate of phenol in a TiO_2 suspension by increasing the partial pressure of O_2 in the bubbled gases.

Reliability of the Quantum Yield of •OH Radical Generation in TiO_2. The major uncertainty in our measurement of the quantum yield of •OH radical generation in TiO_2 is the efficiency of reaction 4 for reaction of •OH radicals on the surface of TiO_2. If this efficiency is less than 93%, our quantum yield could be underestimated. We feel that this is unlikely for three reasons:

(1) In ref 23, we have shown that when the concentration of methanol is increased, the yield of the DMPO−OH spin adduct reaches a plateau above 10 mM. We have used a concentration of 30 mM which is well into the plateau region. Thus there is enough methanol present to saturate reaction 4.

(2) Also in ref 23, we find that the trapping efficiency of •OH radicals by the spin trap DMPO is almost the same between the homogeneous H_2O_2 system and the heterogeneous TiO_2 system. This means that the •OH radicals on the surface of TiO_2 have a similar access to a trapping agent as in the homogeneous solution.

(3) The addition of H_2O_2 caused our measured quantum yield to increase to 0.22. If one can believe that this quantum yield is really 1.0, then our values would be underestimated by a factor of at most 4.5, which we find hard to believe. The findings of Brezova et al.[40] are in agreement with this picture.

There has been some discussion that substrates can be oxidized directly by valence-band holes rather than by hydroxyl radicals generated by reaction 2b. We contend that direct reaction of valence-band holes with organic substrates is only important at very high substrate concentrations. Lepore et al.[8]

found a limiting quantum yield of about unity at very high concentrations of propanal in optically transparent suspension of very small TiO_2 particles. They found that the propanal is strongly adsorbed and the high quantum yields are likely due to direct hole oxidation. Goldstein et al.[41] suggested that at low concentration of phenol, hydroxyl radicals are the primary oxidant, whereas at high concentrations (>0.5 M), photogenerated holes directly oxidize phenol. At the concentration of methanol employed in this work (30 mM), we are convinced that almost all the oxidation of methanol occurs via reaction 4.

5. Conclusions

In this study, a method to measure the quantum yield of •OH radical generation in heterogeneous systems was developed. In the method, a modified integrating sphere, which avoids the interference of scattering light from the particulate system, was used to measure the absorbance of the TiO_2 suspensions, and a ferrioxalate actinometer was used to measure the incident light flux. Accordingly, the flux of absorbed photons could be determined.

The confirmation experiments of the method for the quantum yield measurement were carried out in the *p*-benzoquinone (BQ) and hydrogen peroxide (H_2O_2) systems, whose quantum yields for the *p*-benzosemiquinone ($BQ^{\bullet-}$) and •OH radical generation are well-known. Good agreement with the literature values was obtained, which shows that the method for the quantum yield measurement is reliable.

The primary quantum yield of •OH radical generation in TiO_2 suspensions was determined for the first time to be 0.040 ± 0.003, which provides a basic estimation of the efficiency of the primary process in heterogeneous photocatalysis in this system.

Several effects on the quantum yield were observed. Variation of the TiO_2 loading in the experimental range does not change the quantum yield significantly. The quantum yield changes inversely with the square root of the light intensity. The reduction process has a marked influence on the quantum yield. The addition of the electron acceptor hydrogen peroxide caused a dramatic change of the quantum yield from 0.04 to 0.22, which is the result of changing the reduction rate of the reduction reaction (a rate-controlling process) and inhibiting the recombination of photoinduced electrons and holes. Similar to the addition of H_2O_2, the variation of the O_2 concentration in the solution also changed the rate of the reduction reaction; however, the effect of O_2 concentration on the quantum yield is not as large as the addition of H_2O_2, due to the limitation of adsorption of O_2 on the surface and to its low solubility in water.

Acknowledgment. This work was financially supported by an operating grant from the Natural Sciences and Engineering Research Council. We thank Dr. Aitken R. Hoy for his helpful comments.

Appendix 1

The terms in eq 8 are determined as follows: In general, F_S is given by

$$F_S = \int_{\lambda_1}^{\lambda_2} I_\lambda T_\lambda^f f_\lambda^S \, d\lambda / \int_{\lambda_1}^{\lambda_2} I_\lambda T_\lambda^f \, d\lambda \quad \text{(A1)}$$

where I_λ is the relative incident photon flux in the wavelength band $d\lambda$, T_λ^f is the transmittance of the UV transmitting black filter at wavelength λ, and

$$f_\lambda^S = 1 - 10^{-A_\lambda^S} \quad \text{(A2)}$$

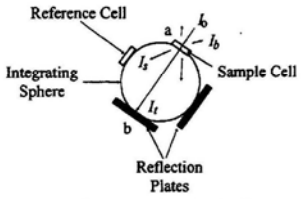

Figure 9. Integrating sphere assembly for the direct measurement of the absorbance of a particle suspension.

is the fraction of light absorbed at wavelength λ, where A_λ^S is absorbance of the sample S at wavelength λ.

The incident photon flux I_o can be determined by a standard actinometer method, based on the photochemical conversion of the ferrioxalate ion into Fe(II), as described by Calvert and Pitts:[23]

$$2Fe(C_2O_4)_3^{3-} \xrightarrow{h\nu} 2Fe^{2+} + 5C_2O_4^{2-} + 2CO_2 \quad \text{(A3)}$$

The generation rate of Fe^{2+} ions $R_{Fe^{2+}}$ (M s^{-1}) can be determined spectrophotometrically at 510 nm after forming a complex with 1,10-phenathroline. The incident photon flux I_o (einstein s^{-1}) is then obtained from

$$I_o = R_{Fe^{2+}}/\phi_{Fe^{2+}} F_{Fe(III)} \quad \text{(A4)}$$

Here $\phi_{Fe^{2+}}$ is the quantum yield of Fe^{2+} generation in the ferrioxalate reaction, and $F_{Fe(III)}$ is the integrated absorption fraction of the ferrioxalate solution over the range of the wavelengths involved in the experiment.

The photon flux I_a absorbed by a sample is

$$I_a = I_o F_S = R_{Fe^{2+}} F_S / \phi_{Fe^{2+}} F_{Fe(III)} \quad \text{(A5)}$$

From eqs A1 and A5 for the wavelength range 300−400 nm

$$I_a = \frac{R_{Fe^{2+}} \int_{300}^{400} I_\lambda T_\lambda f_\lambda^S \, d\lambda}{\phi_{Fe^{2+}} \int_{300}^{400} I_\lambda T_\lambda f_\lambda^{Fe(III)} \, d\lambda} \quad \text{(A6)}$$

According to eq A6, it is necessary, in addition to the measurement of the incident photon flux I_o, that the absorption fraction f_λ^S of the sample in each wavelength band be determined. The integrals in eq A6 were approximated by a sum over the wavelength range 300−400 nm taking a finite bandwidth of 5 nm for each term in the summations.

Appendix 2

The integrating sphere is a useful device to determine the fraction of light absorbed in particulate suspensions.[42] The principle of the integrating sphere is that when incident light, of photon flux I_o, passes through a sample, light, both from that transmitted through the sample and that scattered from the particles, can be completely reflected by an inner highly reflecting surface, composed of very fine $BaSO_4$ particles. The light radiation level in the sphere can then be monitored by a detector.

In a normal measurement using the integrating sphere, a sample cell (0.33 mm path length) is put at position a (as shown in Figure 9) (note that it is important to use a thin cell to avoid losses from the sides). The incident light, of photon flux I_o, passes through the sample, and the transmitted light, of photon flux I_t, and the scattered light from the particles, of photon flux I_S, all influence the reading of the detector in the integrating sphere. The apparent absorbance reading

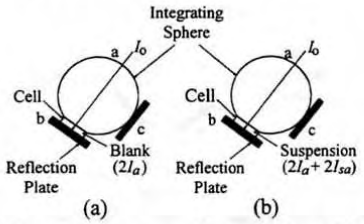

Figure 10. Integrating sphere assembly used in the modified method for the absorbance measurement of a suspension: (a) reference measurement; (b) sample measurement.

A' of the instrument is

$$A' = -\log\left(\frac{I_o - I_s - I_t}{I_o}\right) \tag{A7}$$

But this is not the true absorbance of the sample because the back-scattered light, of photon flux I_b, from the particles is not taken into account in the measurement. Thus a modified method, which avoids this problem, was developed in this study.

In the modified method, a reference solution without particles is put at position b between a reflection plate and the sphere (Figure 10). The instrumental reading A_1 is

$$A_1 \cong -\log\left(\frac{I_o - 2I_a}{I_o}\right) \tag{A8}$$

where I_a is the photon flux absorbed by the homogeneous solution, and the coefficient 2 arises from the fact that the incident light passes through the solution twice, once when the incident light passes through the solution and second back again after it reflects from the reflection plate. Equation A8 assumes a small absorption fraction (I_a/I_o), such that the beam I_o is not significantly attenuated between the incoming path and the outgoing path. In the present case, the absorption fraction is only about 1%, thus this approximation is reasonable. A sample containing a suspension is then put at the same position as that of the homogeneous solution (Figure 10b) and the instrumental reading A_2 is

$$A_2 \cong -\log\left(\frac{I_o - 2I_a - 2I_{sa}}{I_o}\right) \tag{A9}$$

where I_{sa} is the photon flux absorbed by particles in the suspension.

From eqs A8 and A9, the fraction f_λ of light absorbed at wavelength λ by the particles is

$$f_\lambda = \frac{I_{sa}}{I_o} = \frac{10^{-A_1} - 10^{-A_2}}{2} \tag{A10}$$

and the true absorbance A is

$$A = -\log\left(1 - \frac{I_{sa}}{I_o}\right) \tag{A11}$$

References and Notes

(1) Pelizzetti, E.; Minero, C. *Electrochim. Acta* **1993**, *38*, 47.
(2) Fox, M. A.; Dulay, M. T. *Chem. Rev.* **1993**, *93*, 341.
(3) Kamat, P. V. *Chem. Rev.* **1993**, *93*, 267.
(4) Cundall, R. B.; Rudham, R.; Salim, M. *J. Chem. Soc., Faraday Trans. 1* **1976**, *72*, 1642.
(5) Harvey, P.; Rudham, R.; Ward, S. *J. Chem. Soc., Faraday Trans. 1* **1983**, *79*, 1381.
(6) Harvey, P.; Rudham, R.; Ward, S. *J. Chem. Soc., Faraday Trans. 1* **1983**, *79*, 2975.
(7) Schiavello, M.; Augugliaro, V.; Palmisano, L. *J. Catal.* **1991**, *127*, 332.
(8) Lapore, G. P.; Langford, C. H.; Vichova, J.; Vleck, A. Jr. *J. Photochem. Photobiol. A: Chem.* **1993**, *75*, 67.
(9) Valladares, J. E.; Bolton, J. R. In *Photocatalytic Purification and Treatment of Water and Air*; Ollis, D. F., Al-Ekabi, H., Eds.; Elsevier: Amsterdam, 1993; pp 111−120.
(10) Gibson, J. F.; Ingram, D. J. E.; Symons, M. C. R.; Townsend, M. G. *Trans. Faraday Soc.* **1957**, *53*, 914.
(11) Matheson, M. S.; Dorfman, L. M. *Pulse Radiolysis*; MIT Press: Cambridge, MA, 1969.
(12) Asmus, K.-D.; Mockel, H.; Henglein, A. *J. Phys. Chem.* **1973**, *77*, 1218.
(13) Walling, C.; Kato, S. *J. Am. Chem. Soc.* **1971**, *93*, 4275.
(14) Mopper, K.; Zhou, X. *Science* **1990**, *250*, 661.
(15) Zhou, X.; Mopper, K. *Mar. Chem.* **1990**, *30*, 71.
(16) Adams, G. E.; Michael, B. D.; Willson, R. L. Radiation Chemistry. In *Adv. Chem. Ser.*; Gould, R. E., Ed.; American Chemical Society: Washington, DC, 1968; Vol. 81, p 289.
(17) Mopper, K.; Stahovec, W. L. *Mar. Chem.* **1986**, *19*, 305.
(18) Asmus, K.-D.; Wigger, A.; Henglein, A. *Ber. Bunsen-Ges. Phys. Chem.* **1966**, *70*, 862.
(19) Adams, G. E.; Willson, R. L. *Trans. Faraday Soc.* **1969**, *65*, 2981.
(20) Burchill, C. E.; Ginns, I. S. *Can. J. Chem.* **1970**, *48*, 1232, 2628.
(21) Sun, L.; Schindler, K.-M.; Hoy, A. R.; Bolton, J. R. In *Aquatic and Surface Photochemistry*; Helz, G., Zepp, R., Crosby, D., Eds.; CRC Press: Boca Raton, FL, 1994; pp 409−417.
(22) Sun, L. Ph.D. Dissertation, The University of Western Ontario, 1994.
(23) Sun, L.; Hoy, A. R.; Bolton, J. R. *J. Adv. Oxidation Technol.*, in press.
(24) Calvert, J. G.; Pitts Jr., J. N. *Photochemistry*; Wiley: New York, 1967.
(25) Ononye, A. I.; Bolton, J. R. *J. Phys. Chem.* **1986**, *90*, 6270.
(26) Zellner, R.; Exner, M.; Herrmann, H. *J. Atmos. Chem.* **1990**, *10*, 411.
(27) Matthews, R. W.; McEvoy, S. R. *J. Photochem. Photobiol. A: Chem.* **1992**, *64*, 93.
(28) Bahnemann, D.; Henglein, A.; Spanhel, L. *Faraday Discuss. Chem. Soc.* **1984**, *78*, 151.
(29) Anpo, M.; Shima, T.; Kodama, S.; Kubokawa, Y. *J. Phys. Chem.* **1987**, *91*, 4305.
(30) Lin, L.; Al-Thabaiti, S.; Kuntz, R. R. *J. Photochem. Photobiol. A: Chem.* **1992**, *64*, 93.
(31) Kormann, C.; Bahnemann, D. W.; Hoffmann, M. R. *Environ. Sci. Technol.* **1991**, *25*, 494.
(32) This is the usual assumption that is made;[33,34] however, there is no definitive evidence in the literature. For example, Gerischer,[35] in his original theoretical analysis of the kinetics of formation and decay of the transient species in photolyzed TiO_2, *assumed* that the rate constant for reaction 2b is much faster than that for reaction 2c.
(33) Gerischer, H.; Heller, A. *J. Phys. Chem.* **1991**, *95*, 5261.
(34) Hidaka, M.; Kubota, H.; Grätzel, M.; Serpone, N.; Pelizzetti, E. *Nouv. J. Chim.* **1985**, *9*, 67.
(35) Gerischer, H. *Electrochim. Acta* **1993**, *38*, 3.
(36) Tanaka, K.; Hisanga, T.; Rivera, A. P. In *Photocatalytic Purification and Treatment of Water and Air*; Ollis, D. F., Al-Ekabi, H., Eds.; Elsevier: Amsterdam, 1993; pp 169−178.
(37) Wei, T. Y.; Wang, Y. Y.; Wan, C. C. *J. Photochem. Photobiol. A: Chem.* **1990**, *55*, 115.
(38) Linden, L. A.; Rabek, J. F.; Kaminska, A.; Scoponi, M. *Coord. Chem. Rev.* **1993**, *125*, 195.
(39) Okamoto, K.; Yamamoto, Y.; Tanaka, H.; Tanaka, M.; Itaya, A. *Bull. Chem. Soc. Jpn.* **1985**, *58*, 2015.
(40) Brezova, V.; Stasko, A.; Biskupic, S.; Blazkova, A.; Havlinova, B. *J. Phys. Chem.* **1994**, *98*, 8977.
(41) Goldstein, S.; Czapski, G.; Rabani, J. *J. Phys. Chem.* **1994**, *98*, 6586.
(42) Fischer, K. *Beitr. Phys. Atmos.* **1970**, *43*, 244.

JP9505800